Research Article

Wei He and Gang Liao*

Investigation of the early-age performance and microstructure of nano-C–S–H blended cement-based materials

https://doi.org/10.1515/ntrev-2021-0095
received September 5, 2021; accepted September 18, 2021

Abstract: Nano calcium silicate hydrate (nano-C–S–H) has become a novel additive for advanced cement-based materials. In this paper, the effect of nano-C–S–H on the early-age performance of cement paste has been studied, and some micro-characterization methods were used to measure the microstructure of nano-C–S–H-modified cement-based material. The results showed that the initial fluidity of cement paste was improved after addition of nano-C–S–H, but the fluidity gradual loss increased with the dosage of nano-C–S–H. The autogenous shrinkage of cement paste can be reduced by up to 42% maximum at an appropriate addition of nano-C–S–H. The mechanical property of cement paste was enhanced noticeably after adding nano-C–S–H, namely, the compressive strengths were improved by 52% and 47.74% at age of 1 day and 7 days, respectively. More hydration products were observed and pore diameter of cement matrix was refined after adding nano-C–S–H, indicating that the early hydration process of cement was accelerated by nano-C–S–H. This was mainly attributed to seed effect of nano-C–S–H. The detailed relationship between microstructure and early-age performance was also discussed.

Keywords: nano-C–S–H, cement paste, workability, compressive strength, microstructure

1 Introduction

Cement has been invented for more than 100 years and become one of the fundamental building materials in modern society. Generally, the mechanical property of cement paste developed with curing time [1,2]. In practice, the mechanical property of normal cement paste is relatively poor at the early age, which cannot meet the demand of strength, and as a result, the curing and demoulding time must be prolonged, reducing the efficiency of construction and leading to a higher cost. At present, researchers have proposed many solutions to improve the early-age strength of cement paste, such as high-temperature steam curing and addition of early strength agents [3–7]. The high-temperature steam curing method can rapidly improve the early-age strength of cement paste, but it consumes a large amount of energy and produces a mass of greenhouse gases. Moreover, this method is difficult to be widely applied due to its high cost and site limitation [8]. Previous researches have demonstrated that adding a small amount of early strength agent into cement can significantly improve the early-age strength of hardened cement paste. Traditional early strength agents are mainly divided into inorganic and organic category, such as, calcium chloride [9], sodium sulfate [10], and calcium formate [11]. Early strength agent is an additional component for cement hydration system, and it's always challengeable to deal with the compatibility between cement and additives. Traditional early strength agents can effectively improve the early strength of concrete or mortar, but it also brings a series of negative effects. For instance, chloride ions will accelerate the electrochemical corrosion of steel bars and reduce the reliability of concrete structures [12]. The introduction of sodium ions will cause excessive alkalinity in concrete, which will adversely affect the long-term strength of concrete [13,14]. Formate ions have a certain impact on the corrosion resistance and freeze-thaw resistance of concrete [15,16]. In recent decades, scientists have done much work to reduce the negative effects of traditional

* **Corresponding author: Gang Liao,** Department of Traffic and Municipal Engineering, Sichuan College of Architectural Technology, Sichuan, Chengdu 610399, China, e-mail: liaogang@scac.edu.cn
Wei He: Department of Traffic and Municipal Engineering, Sichuan College of Architectural Technology, Sichuan, Chengdu 610399, China

early strength agents, but the situation remains unchanged. Therefore, it's urgent to develop a novel and harmless early strength agent.

Recently, with the development of nanotechnology, some nanomaterials have been introduced into cement to improve its comprehensive performance by regulating the nanostructure [17–20]. For example, nano-SiO_2 is of high activity and can react with $Ca(OH)_2$ easily, generating calcium silicate hydrate (C–S–H), which can promote the secondary hydration of cement and improve the mechanical property and durability of cement-based materials [21,22]. It is well-known that the hydration process of cement is complicated and main hydration products contain C–S–H gel, $Ca(OH)_2$, ettringite, *etc*. In light of avoiding the adverse impact of heterogenous component, some researchers proposed that nano calcium silicate hydrate (nano-C–S–H) should be added into cement to adjust the hydration process at nanoscale [23–26]. Previous works proved that nano-C–S–H can improve the mechanical property of cement-based materials greatly without any risk of electrochemical corrosion or other damages [27]. The mechanism of this enhanced effect of nano-C–S–H has been extensively studied; however, there is no academic viewpoint accepted by all people [28,29]. At present, most researchers tend to support this view that nano-C–S–H is similar in chemical composition and microscopic morphology to C–S–H formed in the hydration reaction, and nano-C–S–H can participate in the hydration reaction as a seed crystal, and thus the nucleation barrier of C–S–H on the heterogenous interface is reduced. Consequently, the hydration rate of cement is accelerated and the mechanical property is improved [28,30,31]. In general, the performance degradation of cement-based materials is usually induced at initial stage, and the early-age performance is vital to the long-term performance. Through summarizing the literatures, it can be found that researchers paid more attention to explain the modification mechanism of nano-C–S–H on cement than to investigate the relationship between the early-age performance and microstructure.

In this paper, the aim is to investigate the effect of nano-C–S–H on the early-age performance of cement paste and figure out the relationship between microstructure and early-age performance including mechanical property and workability. Specifically, the fluidity, autogenous shrinkage, and compressive strength were measured under different addition of nano-C–S–H. And the micromorphology, crystal phases, and pore structure parameters were used to explain the variation of early-age performance. This work may provide a guidance for how to use nano-C–S–H efficiently in improving the early-age comprehensive performance of cement-based materials.

2 Experimental procedure

2.1 Raw materials

Cement used in study was Conch brand P.O. 42.5 cement with specific surface area of 350 m^2/kg and apparent density of 3.15 g/cm^3, and the chemical composition is shown in Table 1. Solid polycarboxylic superplasticizer with water reducing rate of over 30% was used. Nano-C–S–H suspension was a commercial product with a solid content of 20%, purchased from Changan Construction Material Co., Ltd.

2.2 Samples preparation

The water to cement ratio was fixed as 0.36 for all samples, and the content of superplasticizer was 0.025% by mass of cement. And different amounts of nano-C–S–H suspension were added as shown in Table 2. First, 700 g cement and corresponding amount of water were added into the agitator kettle and mixed for 1 min at a low speed mode. And then 0.175 g superplasticizer and corresponding amount of nano-C–S–H were added into the cement paste and mixed for another 1 min at a fast speed mode. Subsequently, the fresh cement paste was casted in the mould (40 mm × 40 mm × 40 mm) and demoulded after one day. At last, samples were cured in a standard room for 3 days and 7 days. The samples were labeled as S-n, where n% stood for the content of solid nano-C–S–H. For instance, S-0.25 meant that the content of solid nano-C–S–H was 0.25% by mass of cement.

Table 1: Chemical composition of cement

Composition	CaO	SiO_2	Al_2O_3	Fe_2O_3	SO_3	MgO	Na_2O	LOI
Mass fraction (%)	59.89	24.06	6.34	3.69	2.46	0.98	0.51	2.07

Table 2: Mix proportions of cement paste

No.	Cement (g)	Water[a] (g)	Nano-C–S–H (g)	Water reducer (g)
S-0	700	252	0	0.175
S-0.25		245	8.75	0.175
S-0.5		238	17.5	0.175
S-0.75		231	26.25	0.175

[a]Water introduced by nano-C–S–H suspension was subtracted.

2.3 Characterization methods

The fluidity of cement paste was measured according to Chinese standard GB/T 8077-2012. After the initial measurement, the fluidity was tested every half an hour until 60 min. The autogenous shrinkage of cement paste was continuously monitored for 7 days by a special apparatus recommended by American standard ASTM C1698. The apparatus was equipped with a bellows (Φ20 mm × 420 mm) and an electronic dial gauge. In a typical test process, the fresh cement paste was poured to the bellow with continuous vibration on a mini-vibrostand until the bellow was filled with cement paste. And then the bellow was laid on a holder with free motion on horizontal. The deformation of the bellow was recorded by an electronic dial gauge. The compressive strength of hardened cement paste was measured according to Chinese standard GB/T 17671-2020. After measuring the compressive strength, the crushed sample was collected and then immersed in absolute ethyl alcohol for 7 days to stop further hydration, and finally, these treated samples were dried at 80°C for micro characterizations. The crystal phases of hydration products were identified with an X-ray diffraction detector (Rigaku, D/max 2550VB/PC) with a Cu Ka ray source operating at 40 kV and 100 mA. The diffraction intensity between 10° and 70° was continuously recorded with the interval of 0.02° at the speed of 4°/min. The pore structure of hardened cement paste was measured by mercury intrusion porosimetry (Quantachrome, Poremaster). Scanning electron microscope (Hitachi, TM4000Plus) was used to observe the micromorphology of hydration products.

3 Results and discussion

3.1 Property of nano-C–S–H

Figure 1(a) shows that the nano-C–S–H suspension was milky white and there was no precipitation, indicating

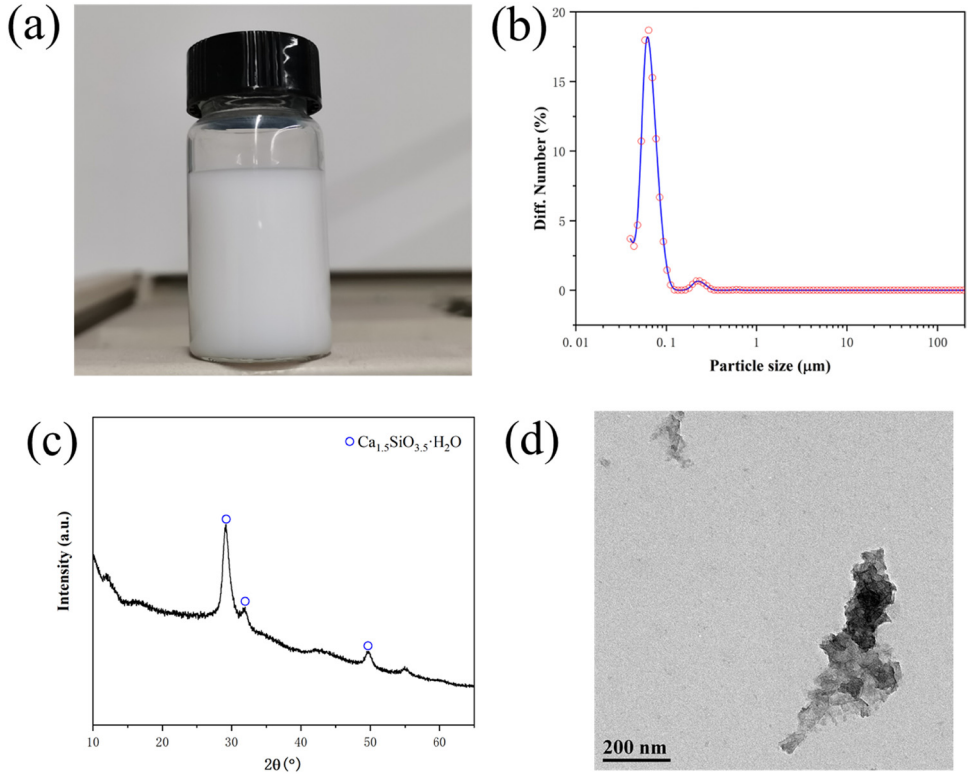

Figure 1: (a) Digital image of nano C–S–H; (b) particle size distribution curve of nano C–S–H; (c) X-ray diffraction pattern of nano C–S–H; and (d) TEM image of nano C–S–H.

that the nano-C–S–H suspension has good dispersion and high stability. Figure 1(b) shows the particle size distribution curve of nano-C–S–H suspension. It can be seen that the particle size of most particles was lower than 100 nm, and the proportion of the particle (about 70 nm) was the highest (18%), suggesting that the nanoparticles in the suspension were well-dispersed. Figure 1(c) is the X-ray diffraction pattern of the solid particles obtained by centrifugal treatment of the suspension, and diffraction peaks at 2θ = 29.355°, 32.053°, and 50.077° were obviously observed, which corresponded to the characteristic diffraction peaks of $Ca_{1.5}SiO_{3.5}{\cdot}H_2O$ according to PDF#33-0306. In Figure 1(d), TEM image of nano-C–S–H is shown, and the particle size was less than 100 nm, which was consistent with the particle size distribution curve. Based on the aforementioned analysis, it can be inferred that the C–S–H nanoparticles adopted in this study had good dispersion, high crystallinity, and good compatibility with Portland cement system.

3.2 Fluidity analysis

Table 3 shows the effect of nano-C–S–H on the fluidity of cement paste. The initial fluidity of cement paste increased continuously with the dosage of nano-C–S–H. When the content of C–S–H increased to 0.5%, the fluidity reached the maximum value of 172.5 mm; however, as nano-C–S–H dosage was over 0.5%, the fluidity did not increase any more, indicating that nano-C–S–H can only improve the initial fluidity of cement paste within a certain range, which may be related to the organic stabilizer in C–S–H suspension. Nanoparticle stabilizers were usually surfactants, which can improve the fluidity of cement paste as an air entraining agent [32]. Specifically, the organic stabilizer has charges on its surface and would be adsorbed on the surface of cement particles, and under the effect of electrostatic repulsion, cement particles would not aggregate, and consequently water would be released and the fluidity of cement is improved. Therefore, the initial fluidity was increased after incorporating nano-C–S–H suspension. As hydration proceeded, the fluidity loss of S-0 was smaller than that of others, and the fluidity gradual loss of the cement paste increased with the content of nano-C–S–H. The fluidity loss rates of S-0.25 at 30 and 60 min were 7.2 and 11.3%, respectively, and the corresponding values of S-0.5 were 8.8 and 16.4%, respectively. The fluidity loss of S-0.75 was close to that of S-0.5, which indicated that the addition of nano-C–S–H can promote the setting process of cement paste. Specifically, the fluidity loss of cement paste was mainly attributed to the formation of C–S–H gel [33], which is a continuous silica tetrahedron network structure and can prevent the flow of hydration products. And the amount of C–S–H gel was determined by the hydration degree of cement, and consequently it can be inferred that the incorporation of nano-C–S–H can promote the hydration process and improve the hydration degree.

Table 3: Fluidity of cement paste added with different dosages of nano-C–S–H

No.	Fluidity (mm)		
	0	30 min	60 min
S-0	105	104	104
S-0.25	132.5	123	117.5
S-0.5	172.5	155.5	143
S-0.75	170	155	142

3.3 Autogenous shrinkage

Figure 2 displays the effect of nano-C–S–H on the autogenous shrinkage of cement paste. It can be seen that the samples held a similar trend in early-age deformation within 7 days. And the autogenous shrinkage process can be approximately divided into three stages. In the first stage (0–5 h), there was a sharp shrinkage, which may be related to the redistribution of water in the solid-liquid system. It can be simply understood from the fact that most water would be rapidly adsorbed by cement particles and the wet cement particles tend to aggregate, thus leading to a huge deformation. The second stage ranged from 5 to 20 h, in which an obvious expansion can be observed. This stage corresponded to the accelerating stage of cement hydration reaction and massive heat would be generated in this stage. Therefore, the volume of cement paste would expand noticeably under the effect of hydration heat [34]. Moreover, a small amount of free CaO in cement reacted with water and produced $Ca(OH)_2$, resulting in a certain micro-expansion. After 20 h of hydration, the shrinkage deformation got into a relatively stable stage and gradually increased with time. This was considered as the sign of autogenous shrinkage of cement paste. It is well-known that autogenous shrinkage is caused by the chemical shrinkage of cement hydration and the self-drying shrinkage inside the cement paste [35]. In the autogenous shrinkage stage, the autogenous shrinkage of S-0.25 was the largest,

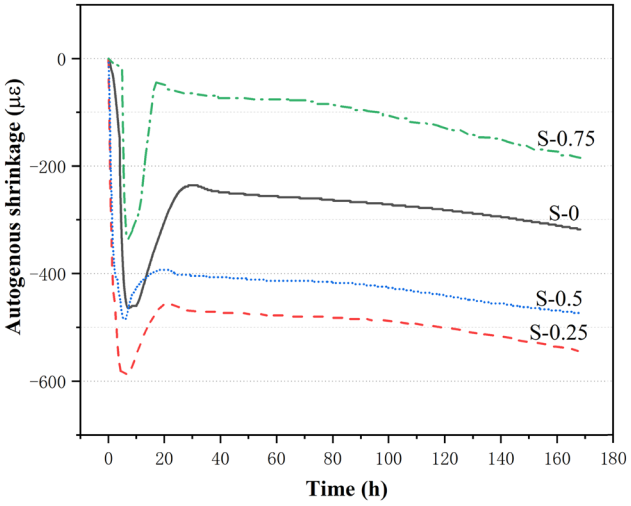

Figure 2: Autogenous shrinkage of cement paste added with different dosages of nano-C–S–H.

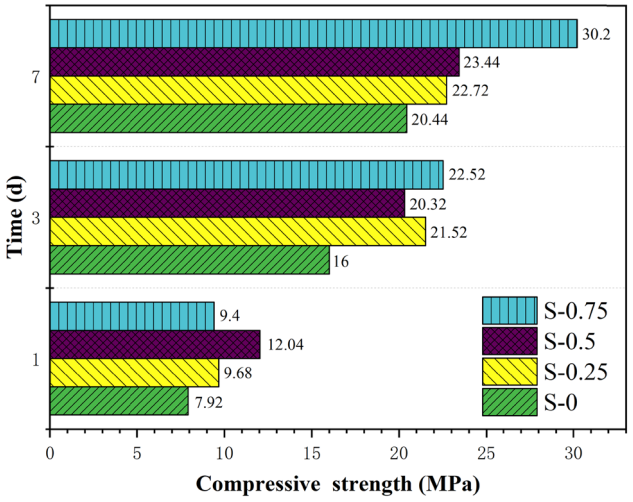

Figure 3: Compressive strength of cement paste added with different dosages of nano-C–S–H.

which reached 550 $\mu\varepsilon$ after 160 h of hydration. The autogenous shrinkage of S-0.5 was lower than that of S-0.25, but much higher than that of S-0. And only the autogenous shrinkage of S-0.75 was lower than that of S-0. Generally, the autogenous shrinkage cement paste is determined by the capillary pressure in pore structure, and capillary pressure is a function of the difference of relative humidity [36]. Moreover, early-age relative humidity can be regarded as an indicator of hydration degree, because faster hydration means larger difference of relative humidity, which will lead to larger autogenous shrinkage. From this perspective, it can be deduced that addition of nano-C–S–H into cement can accelerate hydration reaction and promote the consumption of water, thus reducing the relative humidity and increasing the autogenous shrinkage. And the hydration rate increased with the dosage of nano-C–S–H, so the autogenous shrinkage also increased with nano-C–S–H. However, it should be noticed that the autogenous shrinkage of S-0.75 was much lower than that of S-0. This was probably due to the surfactant component contained in the nano-C–S–H suspension, which can decrease the surface tension of the liquid, thereby reducing the pore pressure [37]. The shrinkage reduction effect of surfactant surpassed the hydration acceleration effect of nano-C–S–H, so the autogenous shrinkage of S-0.75 was the smallest.

3.4 Compressive strength

Figure 3 compares the early-age compressive strength of cement paste in terms of different additions of nano-C–S–H. After incorporation of nano-C–S–H, the mechanical property of all samples was improved. The 1-day compressive strength increased with the content of nano-C–S–H. Among all samples, S-0.5 had the highest strength reaching up to 12.04 MPa, which was increased by 52% compared to S-0, but there was slight decline in strength when the nano-C–S–H content exceeded 5%. According to the strength theory of cement-based materials, the early-age strength of cement paste is determined by the gel to space ratio and micro cracks [38,39]. The 1-day strength indicated that nano-C–S–H can promote the hydration process of cement and produce more hydration products, thus enhancing the gel to space ratio and improving the strength. When the content of nano-C–S–H was excess, the surfactant components in nano-C–S–H suspension were adsorbed on the surface of cement particles, which prevented the migration and diffusion of ions in the cement paste to some extent and thus slowed down the hydration rate of cement. The compressive strength of all samples increased with curing age. The compressive strength of S-0.25 was close to that of S-0.5 at the age of 3 days and 7 days. And the compressive strength of S-0.75 at 7 days was the highest (30.2 MPa) which was 1.48 times higher than that of S-0. This can be explained by the fact that nano-C–S–H can promote hydration of cement, which will pose two effects on the strength of cement paste, namely, increasing gel to space ratio and autogenous shrinkage. Although the gel to space ratio of S-0.75 was close to that of S-0.5, the autogenous shrinkage of S-0.75 was much lower than that of S-0.5 as shown in Figure 2, and therefore the compressive strength of S-0.5 was dramatically reduced by the micro cracks induced by autogenous shrinkage.

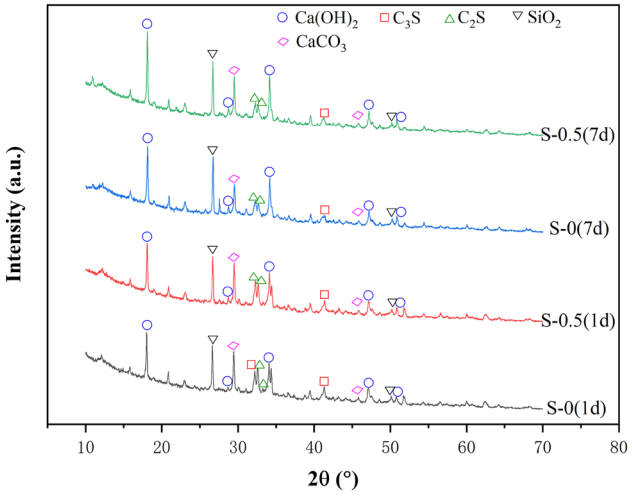

Figure 4: X-ray patterns of hydration products of cement pastes.

3.5 Microstructure

Figure 4 shows the X-ray diffraction patterns of hydration products at different age. During the hydration process (within 7 days), there was little change in the crystal phases of the hydration products, and the main phases were $Ca(OH)_2$ and some unhydrated cement including tricalcium silicate (C_3S) and dicalcium silicate (C_2S). The diffraction intensity of $Ca(OH)_2$ increased with the curing time and the content of nano-C–S–H, indicating that nano-C–S–H had a significant promoting effect on the hydration of cement. However, no diffraction peak of C–S–H was observed, which may be due to the fact that C–S–H gel generated in hydration reaction was amorphous, so there is no diffraction peak. The diffraction intensity of C_3S and C_2S also differed in S-0 and S-0.5, proving that the hydration degree of cement paste was affected by nano-C–S–H. The diffraction peaks of $CaCO_3$ and SiO_2 were observed, which may be caused by the mineral admixtures in clinker.

Figure 5 presents the micromorphology of S-0 and S-0.5 at 1 day. In Figure 5(a), it can be found that S-0 cement matrix was porous and loose, and there were spherical particles distributed homogenously, and a small amount of flocculent substances were formed on the surface of spherical particles. And these flocculent substances were proved to be C–S–H gel by other researchers [40]. Therefore, the further hydration of cement particles was hindered by newly generated C–S–H. This was the main reason that the compressive strength of S-0 was much lower than that of nano-C–S–H-modified samples. In the amplificated image of S-0 as shown in Figure 5(b), needle-rod ettringite can be observed, but the space between

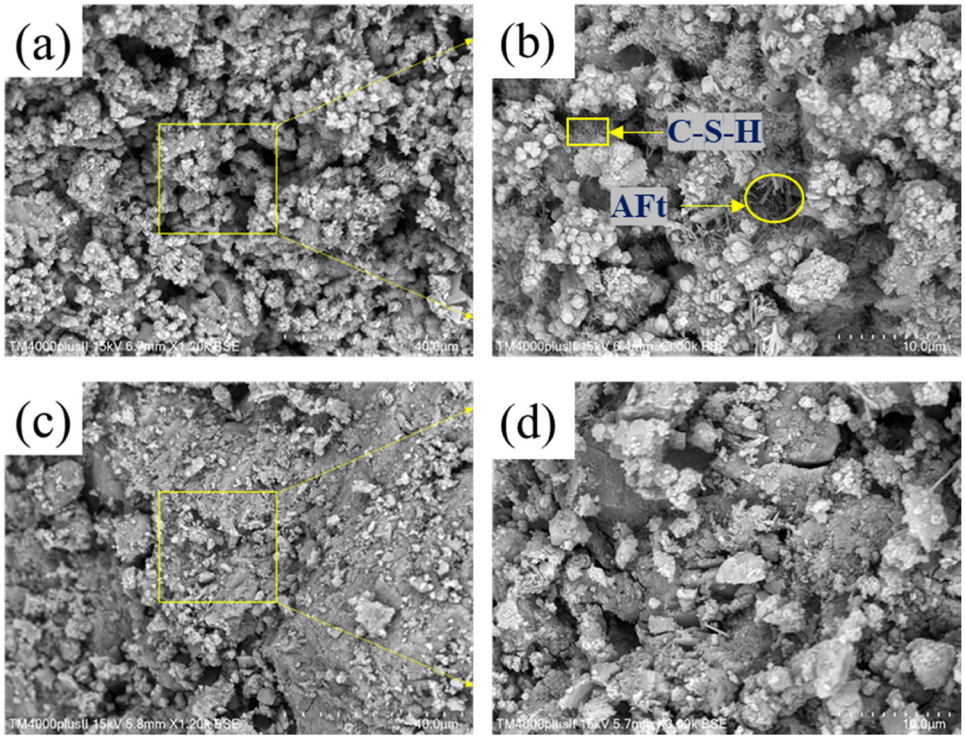

Figure 5: SEM images: (a) S-0 (1 day) amplified factor 1,200; (b) S-0 (1 day) amplified factor 3,000; (c) S-0.5 (1 day) amplified factor 1,200; and (d) S-0.5 (1 day) amplified factor 3,000.

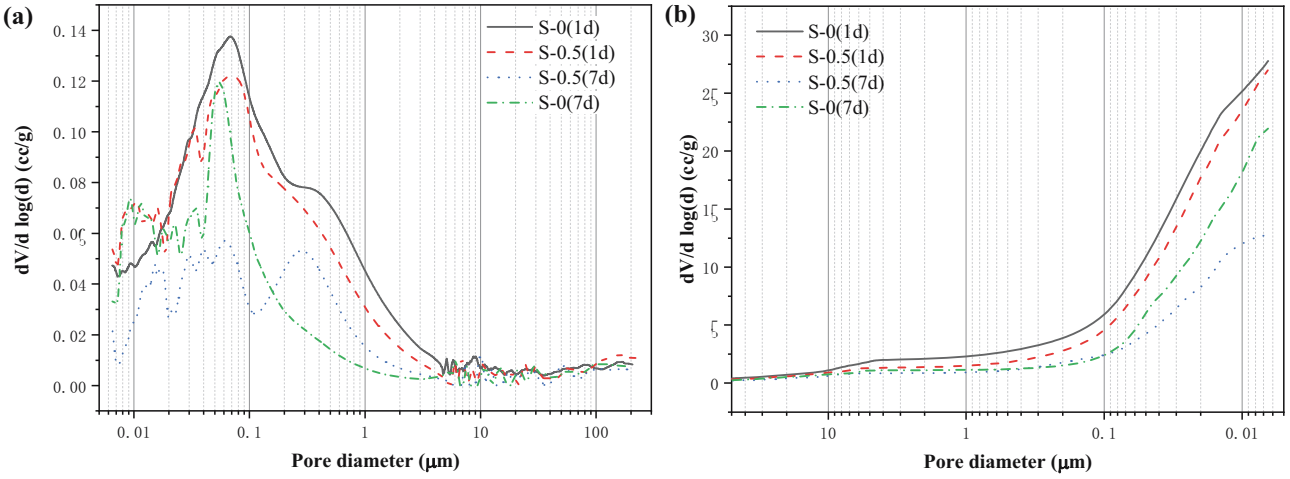

Figure 6: Pore size distribution curves of different cement pastes: (a) differential distribution curves and (b) cumulative distribution curves.

ettringite was not filled by C–S–H gel, leaving many large holes, which was detrimental to the compressive strength of cement paste. The SEM images of S-0.5 are shown in Figure 5(c) and (d). It can be observed that the matrix of S-0.5 was denser than S-0, and no unhydrated clinker particles were observed, and the number of macropores was significantly reduced, indicating that after the incorporation of nano-C–S–H, the hydration rate was significantly accelerated. From the amplificated image of S-0.5, it's clear that the amount of C–S–H gel was increased and the ettringite was wrapped by C–S–H gel closely.

Figure 6 shows the effect of nano-C–S–H on the pore size distribution of cement paste. The pore size of pure cement paste sample S-0 showed an obvious unimodal distribution after 1 day of hydration, and the most probable pore size was about 80 nm. After addition of nano-C–S–H, the most probable pore size of S-0.5 was still 80 nm, but the porosity decreased significantly as show in Table 4, and some smaller pores with diameter between 10 and 80 nm appeared. This can be easily explained by that nano-C–S–H provided more nucleation sites and more hydration products were produced and distributed homogenously, and consequently the macro pores were filled by C–S–H gel and more nanopores were generated inside C–S–H gel, which is not detrimental to the mechanical property of cement-based materials. The porosity of S-0 and S-0.5 samples decreased with hydration time. S-0 still presented a unimodal distribution at the age of 7 days and the most probable pore size decreased to 60 nm, but the pore size distribution range was narrowed. S-0.5 displayed a multimodal distribution and its porosity was the lowest after 7 days of hydration, and additionally the pore size distribution became more complicated. In Table 4, it can be seen that the porosity of cement pastes was noticeably reduced after adding nano-C–S–H at the same hydration age. The pore structure information directly proved that the porosity was refined after adding nano-C–S–H, that is, the macro pores were filled with hydration products and more micropores were produced inside the C–S–H gel.

Table 4: Most probable pore size and porosity of cement pastes

	S-0 (1 day)	S-0.5 (1 day)	S-0 (7 days)	S-0.5 (7 days)
Pore diameter (nm)	80	80	50	60
Total porosity[a] (%)	19.1079	10.4291	7.2781	4.5354

[a] Total porosity consists of intraparticle and interparticle porosity.

4 Conclusion

In summary, nano-C–S–H suspension can improve the initial fluidity of cement paste, and the fluidity gradual loss rate increased with the dosage of nano-C–S–H, reaching up to 16.4% at 60 min. The autogenous shrinkage of cement paste decreased with the content of nano-C–S–H, and the sample with addition of 0.75% nano-C–S–H by mass of cement had the smallest autogenous shrinkage (184 $\mu\varepsilon$), which was even lower than that of pure cement paste (317 $\mu\varepsilon$). Overall, the compressive strength of samples increased with the content of nano-C–S–H and curing time, and the sample doped with 0.75% nano-C–S–H by mass of cement had the highest compressive strength at 7 days (30.2 MPa), which was about 1.48 times higher than that of pure cement paste. This enhanced effect was attributed to the reduction of gel to space ratio

and less micro cracks induced by addition of appropriate amount of nano-C–S–H. Microstructure results confirmed that the early hydration reaction of cement was promoted by nano-C–S–H, and nano-C–S–H provided massive nucleation sites and accelerated the mass transfer process, and thus more hydration products were produced. The pore structure was refined by these C–S–H gel, leading to a cement matrix of low porosity and less defect.

Funding information: This research was funded by Deyang Science and Technology Program (No. 2020SZZ047, No. 2019SZ083).

Author contributions: All authors have accepted responsibility for the entire content of this manuscript and approved its submission.

Conflict of interest: The authors state no conflict of interest.

References

[1] Rodrigues FA, Joekes I. Cement industry: sustainability, challenges and perspectives. Environ Chem Lett. 2011;9:151–66.
[2] Schneider M, Romer M, Tschudin M, Bolio H. Sustainable cement production – present and future. Cem Concr Res. 2011;41:642–50.
[3] Shi J, Liu B, Zhou F, Shen S, Dai J, Ji R, et al. Heat damage of concrete surfaces under steam curing and improvement measures. Constr Build Mater. 2020;252:119104.
[4] Liu B, Jiang J, Shen S, Zhou F, Shi J, He Z. Effects of curing methods of concrete after steam curing on mechanical strength and permeability. Constr Build Mater. 2020;256:119441.
[5] Yuan X, Li B, Cui G, Zhao S, Zhou M. Effect of fly ash and early strength agent on durability of concrete exposed to the cyclic sulfate environment. J Wuhan Univ Techno-Mater Sci Ed. 2010;25:1065–9.
[6] Wang H, Zhang S, Wu B. Experimental study on selection of early-strength agent for low-strength cementitious materials prepared with manganese tailings. Environ Earth Sci. 2018;77:231.
[7] Liu C, Liu Y, Liu Z, Hu C, Huang X, Yang L, et al. Heat-cured concrete: improving the early strength and pore structure by activating aluminosilicate internal curing agent with triisopropanolamine. J Am Ceram Soc. 2019;102:6227–38.
[8] Rajhans P, Chand G, Kisku N, Panda SK, Nayak S. Proposed mix design method for producing sustainable self compacting heat cured recycled aggregate concrete and its microstructural investigation. Constr Build Mater. 2019;218:568–81.
[9] Torkittikul P, Chaipanich A. Optimization of calcium chloride content on bioactivity and mechanical properties of white Portland cement. Mater Sci Eng: C. 2012;32:282–9.
[10] Zou F, Hu C, Wang F, Ruan Y, Hu S. Enhancement of early-age strength of the high content fly ash blended cement paste by sodium sulfate and C–S–H seeds towards a greener binder. J Clean Prod. 2020;244:118566.
[11] Heikal M. Effect of calcium formate as an accelerator on the physicochemical and mechanical properties of pozzolanic cement pastes. Cem Concr Res. 2004;34:1051–6.
[12] Choi Y-S, Kim J-G, Lee K-M. Corrosion behavior of steel bar embedded in fly ash concrete. Corros Sci. 2006;48:1733–45.
[13] Türkmen İ, Gavgalı M. Influence of mineral admixtures on the some properties and corrosion of steel embedded in sodium sulfate solution of concrete. Mater Lett. 2003;57:3222–33.
[14] She A, Ma K, Zhao P, Wang J. Characterization of calcium aluminate cement hydration: comparison of low-field NMR and conventional methods. Adv Cem Res. 2021;1–24.
[15] Shi X, Fay L, Peterson MM, Yang Z. Freeze–thaw damage and chemical change of a portland cement concrete in the presence of diluted deicers. Mater Struct. 2010;43:933–46.
[16] Xu J, Tang YH, Wang XZ. A correlation study on optimum conditions of microbial precipitation and prerequisites for self-healing concrete. Process Biochem. 2020;94:266–72.
[17] Liu X, Jiang B, Liao G, Zuo J, Xu J, Shah SP. Research on the smart behavior of MCNT grafted CF/cement-based composites. Fullerenes, Nanotubes Carbon Nanostruct. 2021;29:1–8.
[18] Liu X, Liao G, Zuo J. Enhanced thermoelectric properties of carbon fiber-reinforced cement composites (CFRCs) utilizing Bi_2Te_3 with three doping methods. Fullerenes, Nanotubes Carbon Nanostruct. 2020;29:1–9.
[19] Fakharpour M, Karimi R. Electromagnetic wave absorption properties of MWCNTs-COOH/cement composites with different shapes of chiral, armchair and zigzag. Fullerenes, Nanotubes Carbon Nanostruct. 2021;29:386–93.
[20] Jia Z, Wei J, Wang Y, Jiang Y, Zhang H. Enhanced thermoelectric properties of cement-based composites by Cl_2/HNO_3 pretreatment of graphene. Fullerenes, Nanotubes Carbon Nanostruct. 2021;1–9.
[21] Jo B-W, Kim C-H, Tae G-H, Park J-B. Characteristics of cement mortar with nano-SiO_2 particles. Constr Build Mater. 2007;21:1351–5.
[22] Zhu Z, Wang Z, Zhou Y, Chen Y, Zhou L, She A. Evaluation of the nanostructure of calcium silicate hydrate based on atomic force microscopy-infrared spectroscopy experiments. Nanotechnol Rev. 2021;10:807–18.
[23] Wang F, Kong X, Jiang L, Wang D. The acceleration mechanism of nano-C–S–H particles on OPC hydration. Constr Build Mater. 2020;249:118734.
[24] Land G, Stephan D. The effect of synthesis conditions on the efficiency of C–S–H seeds to accelerate cement hydration. Cem Concr Compos. 2018;87:73–8.
[25] Pedrosa HC, Reales OM, Reis VD, Paiva MdD, Fairbairn EMR. Hydration of Portland cement accelerated by C–S–H seeds at different temperatures. Cem Concr Res. 2020;129:105978.
[26] Xu J, Wang BB, Zuo JQ. Modification effects of nanosilica on the interfacial transition zone in concrete: A multiscale approach. Cem Concr Compos. 2017;81:1–10.
[27] He W, Liao G. Effects of nano-C–S–H seed crystal on early-age hydration process of Portland cement. Fullerenes, Nanotubes Carbon Nanostruct. 2021;1–8.

[28] Wang F, Kong X, Jiang L, Wang D. The acceleration mechanism of nano-CSH particles on OPC hydration. Constr Build Mater. 2020;249:118734.
[29] John E, Epping JD, Stephan D. The influence of the chemical and physical properties of CSH seeds on their potential to accelerate cement hydration. Constr Build Mater. 2019;228:116723.
[30] Das S, Ray S, Sarkar S. Early strength development in concrete using preformed CSH nano crystals. Constr Build Mater. 2020;233:117214.
[31] Puligilla S, Chen X, Mondal P. Does synthesized C–S–H seed promote nucleation in alkali activated fly ash-slag geopolymer binder? Mater Struct. 2019;52:65.
[32] Mendes JC, Moro TK, Figueiredo AS, do Carmo Silva KD, Silva GC, Silva GJB, et al. Mechanical, rheological and morphological analysis of cement-based composites with a new LAS-based air entraining agent. Constr Build Mater. 2017;145:648–61.
[33] Wang L, Yang HQ, Zhou SH, Chen E, Tang SW. Hydration, mechanical property and C–S–H structure of early-strength low-heat cement-based materials. Mater Lett. 2018;217:151–4.
[34] Maruyama I, Teramoto A, Igarashi G. Strain and thermal expansion coefficients of various cement pastes during hydration at early ages. Mater Struct. 2014;47:27–37.
[35] Wu L, Farzadnia N, Shi C, Zhang Z, Wang H. Autogenous shrinkage of high performance concrete: a review. Constr Build Mater. 2017;149:62–75.
[36] Yang L, Shi C, Wu Z. Mitigation techniques for autogenous shrinkage of ultra-high-performance concrete – a review. Compos Part B: Eng. 2019;178:107456.
[37] Gong J, Zeng W, Zhang W. Influence of shrinkage-reducing agent and polypropylene fiber on shrinkage of ceramsite concrete. Constr Build Mater. 2018;159:155–63.
[38] Pichler B, Hellmich C, Eberhardsteiner J, Wasserbauer J, Termkhajornkit P, Barbarulo R, et al. Effect of gel–space ratio and microstructure on strength of hydrating cementitious materials: an engineering micromechanics approach. Cem Concr Res. 2013;45:55–68.
[39] Khan M, Ali M. Use of glass and nylon fibers in concrete for controlling early age micro cracking in bridge decks. Constr Build Mater. 2016;125:800–8.
[40] She A, Ma K, Liao G, Yao W, Zuo J. Investigation of hydration and setting process in nanosilica-cement blended pastes: In situ characterization using low field nuclear magnetic resonance. Constr Build Mater. 2021;304:124631.